Chalcogenide Letters Vol. 20, No. 3, March 2023, p. 187 - 196

Physical properties of Mg doped ZnS thin films via spray pyrolysis

R. S. Ali[a,*], H. S. Rasheed[b], N. D. Abdulameer[c], N. F. Habubi[d], S. S. Chiad[b]
[a]*Department of Physics, College of Science, Mustansiriyah University, Baghdad, Iraq*
[b]*Department of Physics, College of Education, Mustansiriyah University, Baghdad, Iraq*
[c]*Department of Optics Techniques, Al-Mustaqbal University College, Babylon, Iraq*
[d]*Department of Engineering of Refrigeration and Air Conditioning Technologies, Alnukhba University College, Baghdad, Iraq*

Chemical spray pyrolysis (CSP) was utilized to create pure Zinc Sulfide (ZnS) and magnesium (Mg) doped thin films on a clean glass substrate at a temperature equal to 400°C. X-ray diffraction test revealed a cubic wurtzite crystal structure with average crystallite sizes of 10.99 and 12.27 nm for ZnS and ZnS: Mg, respectively. XRD analysis of the doped films revealed a polycrystalline structure with a predominant peak along the (220) plane and additional peaks along the (111), (200), and (222) planes. The grain size raised from 10.99 to 12.27 nm as a result of the XRD patterns. The increase in Mg content from 0% to 3%, affect the bandgap that fell from 3.52 to 3.42 eV. As the Mg content increased, the transmittance and refractive index of the films was lowered.

(Received December 12, 2022; Accepted March 3, 2023)

Keywords: ZnS thin films, Mg, XRD, AFM

1. Introduction

ZnS is a semiconductor that assigned to the II-VI family. It has an n-type conductivity and a direct bandgap ranges from 3.40 to 3.74 eV when measured at ambient temperature [1]. It has a high refractive index, which enables it to be highly transparent in VIS and near-IR spectra [2]. Only at ambient temperature does the cubic ZnS phase remain stable; at higher temperatures, it changes to the hexagonal phase [3]. The incorporation of particular dopants into the lattice of a semiconductor chalcogenide can result in a modulation of the material's chracterizaions [4]. Doping is the intentional addition of another kind of atoms to an element or composition in order to make useful changes in its properties. Useful way of controlling electrical conductivity and other magnetic and optical properties is combining doping and crystal defects procedure [5]. Mg-containing II–VI semiconductors, for example, have been employed in optoelectronic devices [6]. Magnesium is an excellent doper element for substituting Zn in its lattice and bridging bandgap in the ultraviolet area because its radius is comparable to that of the Zn2+(0,60 A) ion [7, 8]. Due to its comparable ionic radius to that of zinc and its history of utilization as an eco-friendly phosphor encompasses a diverse spectrum of economic sectors, magnesium was selected as the dopant material for this particular research project. [10]. To make ZnS thin films, microwave-assisted [11], hydrothermal [12], MBE, PLD [13, 14] CBD [15], sputtering [16], and CSP [17-20] have all been used. CSP has received a lot of attention as a technology because of its capacity to deposit over a large region, low cost, and ambient operating environment. Throughout the last decade, CSP has consistently detailed pure and doped ZnS, as well as their uses, for ZnS thin film production [21].

* Corresponding author: reemphy81@uomustansiriyah.edu.iq
https://doi.org/10.15251/CL.2023.203.187

2. Experimental

Thin films of ZnS and ZnS: Mg were deposited using an in-built spray pyrolysis coating machine; the quality of these films was good when generated by spray. To prepare the spray solution, dissolve the needed amount of zinc chloride (ZnCl2) in deionized water. In order to obtain Ag doping, Mg trichloride ($MgCl_3$) was dissolved in isopropyl alcohol and added to the precursor solution. The spray solution volume was 50 ml and the doping concentration was (0, 1, 3) percent. The following are the prerequisites for preparation: The spraying interval was increased by 85 s to minimize cooling, and the spray rate was 5 mL/min with nitrogen gas as the carrier gas. Using a weighing method, the film thickness was determined to be 340± 25 nm. A UV-visible Shimadzu twin beam spectrophotometer was used to obtain optical transmittance. XRD was utilized to ascertain the fundamental characteristics of the film's structure, and AFM was used to study film surface.

3. Physical characterization

3.1. Properties of the structure

Figure 1 shows XRD of the intended films produced at 400°C. Scanning 2 with a grazing angle of 10^o–70^o. In all the films, the basic peaks were (111), (200), (220), and (222) planes were assigned to the 28.52°, 33.07°, 47.52°, and 59.12°, respectively.

The XRD pattern, however, showed no peak that belonged to MgO, metallic Zn, and Mg. Because the radius of the Mg^{2+} ion is smaller than that of the Zn^{2+} ion, Mg doping resulted in a modest increase in the (220) peak, showing that the crystal structure of ZnS was altered by the Mg^{2+} ion substitution. [22, 23] reported a similar effect. The Scherrer formula [24, 25] is utilized to obtain the grain sizes (D) of the films quantitatively:

$$D = \frac{k\lambda}{\beta cos\theta} \tag{1}$$

β is FWHM calculated in radians. For the CuKa line, k equal to 0.94. Table contains the values for D. of magnesium-doped ZnS thin films is lower than that of pure ZnS. Because Mg^{2+} has a smaller ionic radius than Zn^{2+}, it tends to occupy interstitial positions, compacting the unit cell [26].

A dislocation is a crystallographic fault or imperfection that occurs inside a crystal structure. Several material properties are affected by the presence of dislocations [27]. The density of dislocations was calculated employing the formula [28, 29]:

$$\delta = \frac{1}{D^2} \tag{2}$$

Microstrain (ε) of films was deduced by using the following equation [30, 31]:

$$\varepsilon = \frac{\beta cos\theta}{4} \tag{3}$$

As grain size grows, $\delta \; and \; \varepsilon$ decrease, indicating better crystallinity. Same findings are published by Hasanzadeh [32, 33]. Figure 2 depicts the structural characteristics S_P of thin ZnS and ZnS:Mg films.

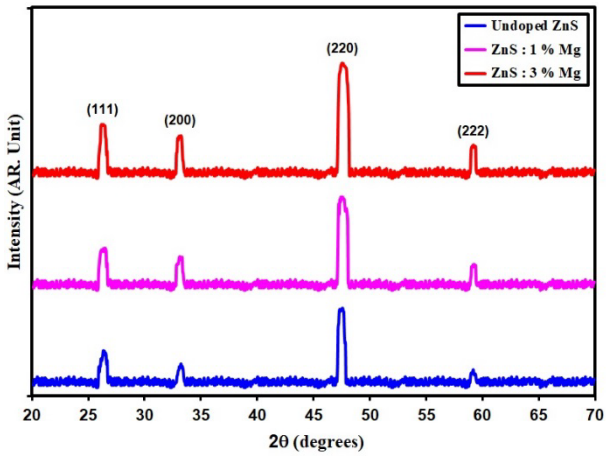

Fig. 1. XRD styles of grown films.

Table 1. D, optical bandgap and S_P of grown films.

Samole	2 θ (°)	(hkl) Plane	FWHM (°)	E_g (eV)	D (nm)	δ(× 10^{15}) (lines/m^2)	Strain (× 10^{-3})
Undoped ZnS	47.52	220	0.79	3.52	10.99	8.27	3.15
ZnS: 1% Mg	47.49	220	0.75	3.47	11.57	7.47	2.99
ZnS: 3% Mg	47.46	220	0.71	3.42	12.27	6.69	2.83

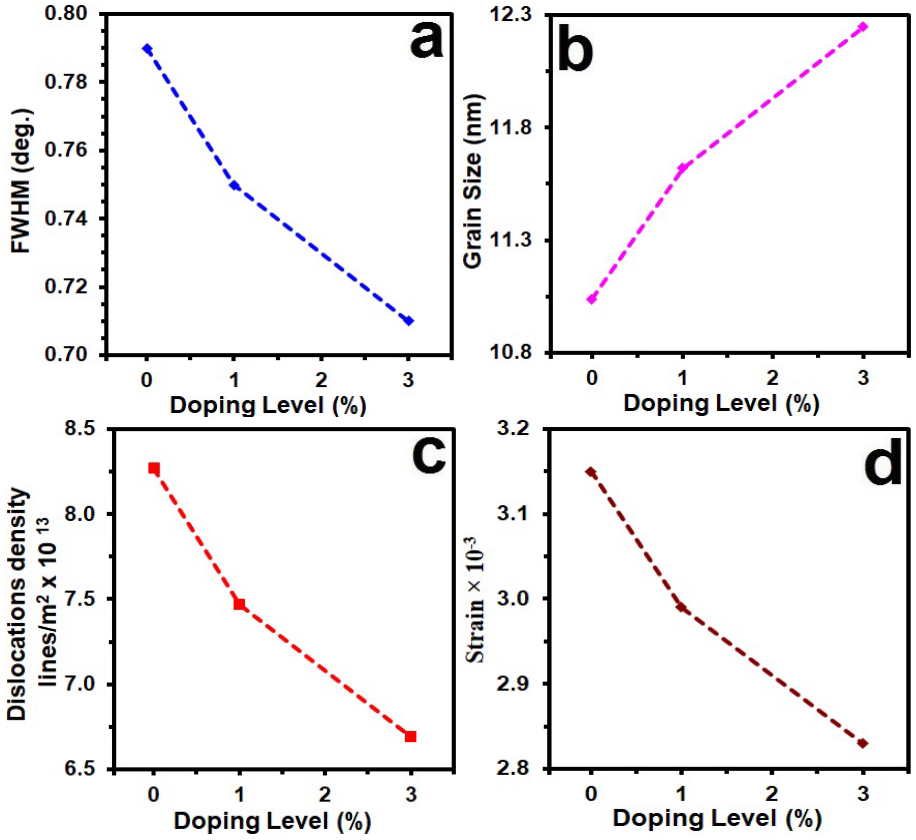

Fig. 2. FWHM (a) D (b) δ (c) ε (d) of the grown films.

3.2. AFM measurements

The films have a consistent appearance, are tightly packed, and do not contain any pinholes; this suggests that their morphology has a limited number of grain sizes, and the fact that they are uniformly scattered suggests that they are crystalline. The deposited layer appears dense and clings well to the substrate at first glance. There was no sign of a crack. The particle size P_s range was 61.15 to 48.57 nanometers. When the Mg ratio is increased, however, P_s sizes shrink, as shown in Table 2. Figure 3 depicts the films' surface roughness R_a and Root Mean Square (RMS).

Deviation of the profile from the average height [34]. As the Mg ratio rises, the surface roughness and RMS values fall, indicating that the grain size shrinks. The information in Table 2 and Figure 3 is identical. Lowers in P_s is thought to be caused by Mg atoms in the interstitial portions of ZnS, as well as the breaking of ZnS bonds [35].

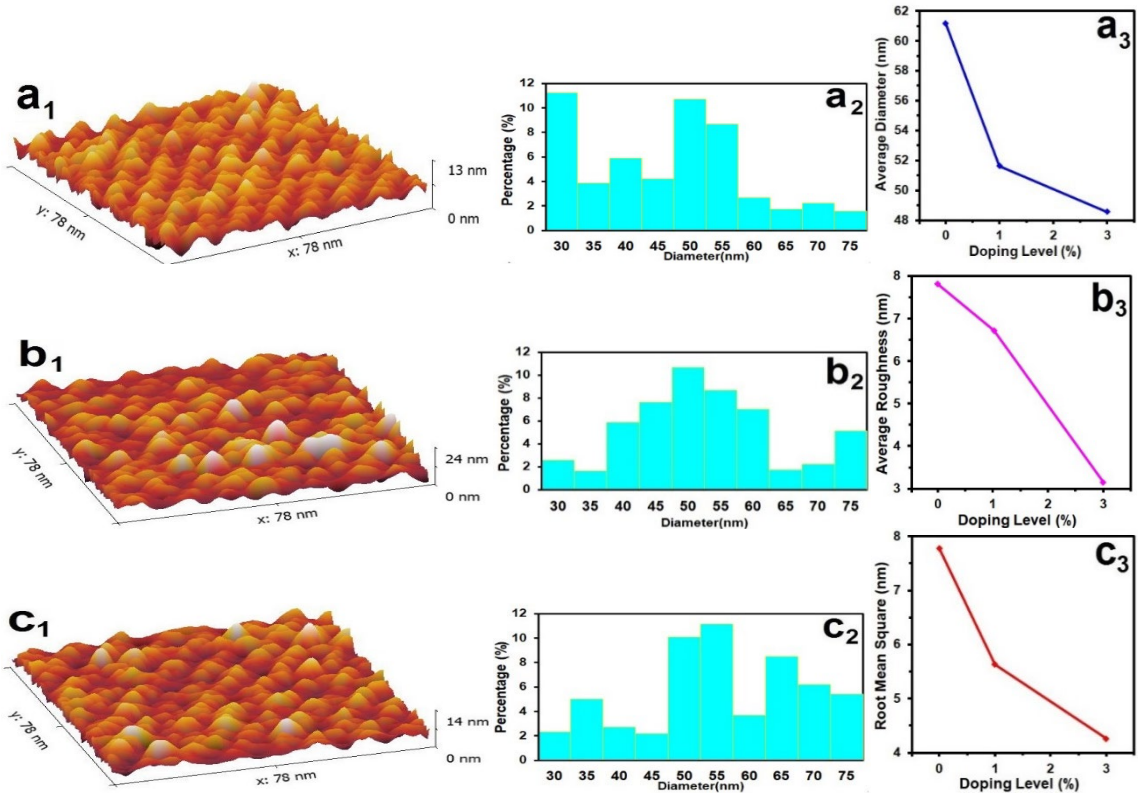

Fig. 3. AFM images and parameters.

Table 2. AFM parameters of the intended films.

Samples	P_s nm	R_a (nm)	R. M. S. (nm)
Undoped ZnS	61.15	7.81	7.78
ZnS: 1% Mg	51.64	6.73	5.63
ZnS: 3% Mg	48.57	3.15	4.26

3.3. Optical properties

Transmitting and absorbing spectrum of ZnS and ZnS:Mg thin films were observed in the UV-visible near infrared ranges (300-900) nm. Figure 4 depicts how the transmittance of as-deposited ZnS thin films, as well as pure and doped samples, fluctuates in the UV-visible region. When doped with 3 percent Mg, the film's transmittance reduced to 65 percent. The decrease in

transmittance may be due to the successful integration of dopant atoms into the ZnS lattice [36, 37].

Absorption coefficient α was calculated from [38, 39]:

$$\alpha = 2.303\frac{A}{d} \tag{4}$$

where (A) refers to the absorption and (d) is film thickness. The fluctuation of α with wavelength is offered in (Fig. 5). It is seen a higher α in the UV region, which then reduces suddenly and becomes nearly constant in the vis-NIR range. A considerable raise in absorption coefficient with increasing Mg concentration in ZnS samples indicates improved optical absorption in the UV band. All of the films had high absorption coefficients (10^5 m^{-1}), which are consistent with previous research. [40].

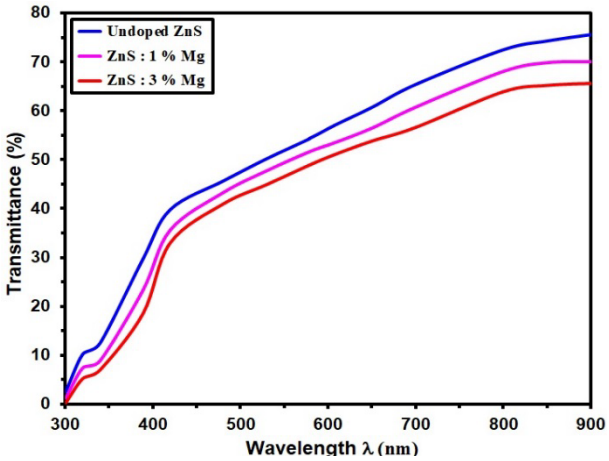

Fig. 4. Transmittance of the intended films.

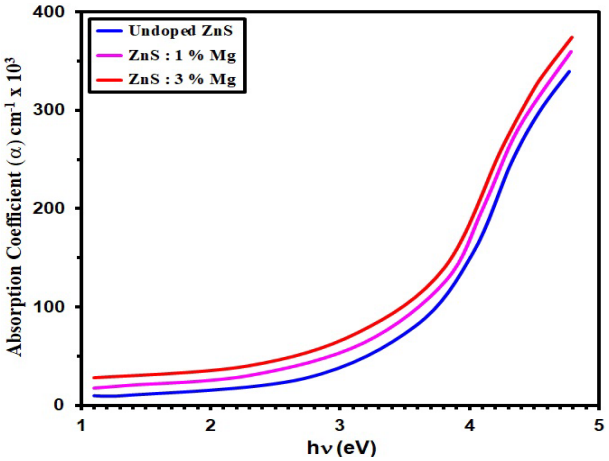

Fig. 5. Absorption coefficient spectra of pure and ZnS:Mg thin films. with various doping.

The optical band gap $E_{g\ of}$ the samples is calculated employing equation (5) [41,42]:

$$\alpha h\nu = A(h\nu - E_g)^{\frac{1}{2}} \tag{5}$$

where A is constant.

Calculation of E_g is done by using the intercept of estimating graph of $(h\nu)^2$ versus photon energy (hν) (Fig. 6). Based on estimating of the plot, E_g of ZnS is 3.52eV. After doping 1 percent

and 3 percent Mg, it has changed to 3.47eV and 3.42eV, respectively. The band gap of ZnS:Mg vs. Mg content is depicted in Figure 5. When demonstrated in this diagram E_g as the Mg content increases from 1% to 3%. The Mg doped concentration grows in proportion to the grade of the crystal. Increased Mg doping is likely to cause lattice deformation and defects in crystals. The inclusion of Mg in the ZnS texture regards the purpose of the development of additional collection centers due to low emission energy (shrinkage effect) [43, 44].

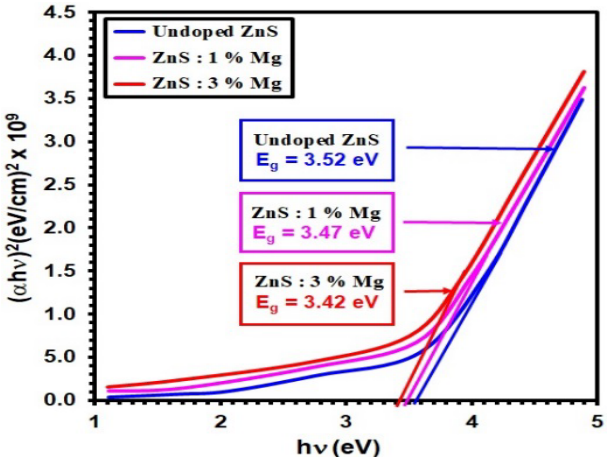

Fig. 6. E_g of the intended films.

Equation (6) was used to calculate refractive index (n) [45, 46]:

$$R = \frac{(n-1)^2}{(n+1)^2} \tag{6}$$

where reflectance represented by (R). It is calculated by using equation (7).

$$A + R + T = 1 \tag{7}$$

The extinction coefficient (k) was studied by using equation (8) [47, 48]:

$$k = \frac{\alpha\lambda}{4\pi} \tag{8}$$

Figure 7 shows that at 400°C, the refractive index and extinction of samoles are lower than doped films at 1% and 3%. The refractive index decreased as the wavelength increased, eventually flattening out at longer wavelengths, showing normal dispersion behavior [49-51].

When refractive index of a material increases, so does reflection. In the 700-900 nm wavelength range, the films' extinction coefficients were around zero, which matches the transmittance spectra in Figure 8. As λ increases, k drops. The absorption values of a material determine its extinguishment coefficient.

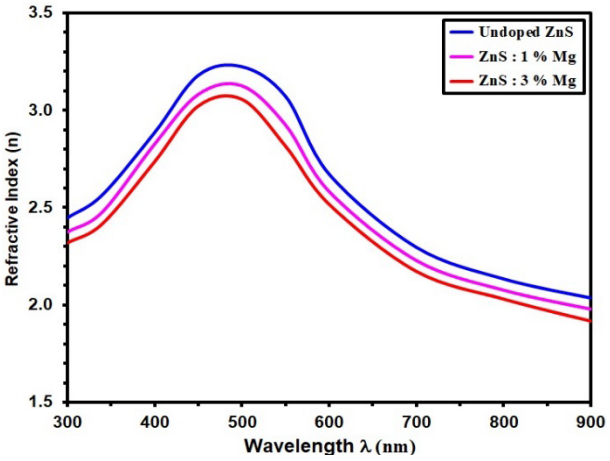

Fig. 7. Refractive index of the intended films.

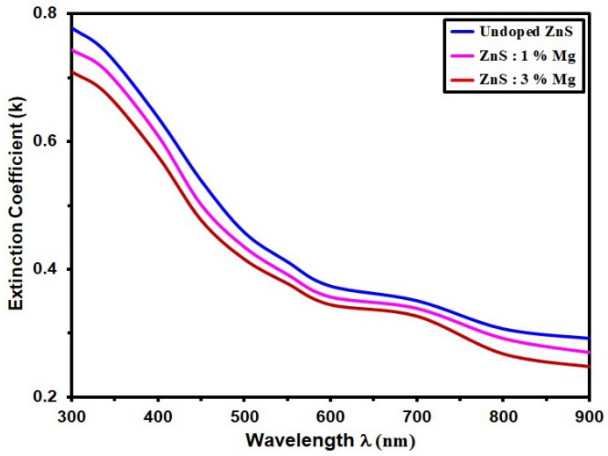

Fig. 8. Extinction coefficient spectra of pure and ZnS: Mg thin films with various doping.

4. Conclusion

Chemical spray pyrolysis was utilized to make ZnS and ZnS: Mg samples with varying concentrations of Mg doping at bases heated to 400°C. XRD spectra were used to examine the effect of Mg on the structural features of ZnS films. Mg doping was calculated in the (10.99-12.27)nm range, and all of the generated films are nanocrystalline. With increasing Mg doping concentration, topographical examination of the film surface revealed a decrease in practical size. With increasing Mg content, the band gap energy reduced from 3.52 eV to 3.42 eV, according to optical properties.

Acknowledgments

Researchers are grateful to Mustansiriyah University (www.uomustansiriyah.edu.iq) and Alnukhba University College.

References

[1] Y. P. Venkata Subbaiah, P. Prathap, K.T. Ramakrishna Reddy, Applied Surface Science, 253, 2409(2006).
https://doi.org/10.1016/j.apsusc.2006.04.063
[2]S. H. Deulkar, C. H. Bhosaile, M. Sharon, J. Phys. Chem. Solids 65, 1879(2004).
https://doi.org/10.1016/j.jpcs.2004.06.012
[3] X. Fang, T. Zhai, U.K. Gautam, L. Li, L. Wu, Y. Bando, D. Golberg, Progr. Mater. Sci. 56, 175 (2011).
https://doi.org/10.1016/j.pmatsci.2010.10.001
[4] S.V. Nistor, M. Stefan, L.C. Nistor, E. Goovaerts, G. Van Tendeloo, Phys. Rev. B 81, 035336 (2010).
https://doi.org/10.1103/PhysRevB.81.035336
[5] R. Jothi Ramalingam, A. K. Shukla, K. Kombaiah, J. J. Vijaya, A. M.Tawfeek, Optik (Stuttg). 148, 325-331(2017).
[6] R. Ghosh and D. Basak, J Appl. Phys;101:0-6(2007).
https://doi.org/10.1016/j.ijleo.2017.08.129
[7] Y. Hu., B. Cai, Z. Hu, Y. Liu, S. Zhang and H. Zeng, Curr Appl Phys;15:4230-8(2015).
[8]A.S. Dive, K.P. Gattu, N.P. Huse, D.R. Upadhayay, D.M. Phase, R.B. Sharma, Mater. Sci. Eng., B 228, 91 (2018).
[9] Q. Shi, Z. Wang, Y. Liu, B. Yang, G. Wang, W. Wang, J. Zhang, J. Alloys Compd. 553, 172 (2013).
https://doi.org/10.1016/j.jallcom.2012.11.135
[10] T.T. Quynh Hoa, L.V. Vu, T. Dinh Canh, N. Ngoc Long, J. Phys: Conf. Ser. 187, 012081 (2009).
https://doi.org/10.1088/1742-6596/187/1/012081
[11] H. Yang, Ch. Huang, X. Su and A. Tang, J. Alloy.Compd. 402, 274-277 (2005).
https://doi.org/10.1016/j.jallcom.2005.04.150
[12] T.T. Quynh Hoa, L.V. Vu, T. Dinh Canh and N. Ngoc Long, J. Phys: Conf. Ser. 187, 012081 (2009).
https://doi.org/10.1088/1742-6596/187/1/012081
[13] M. Yokoyama, K.-i. Kashiro and S.-i. Ohta, Appl. Phys. Lett.,49, 411(1986).
https://doi.org/10.1063/1.97604
[14] S. Yana, R. Schroeder, B. Ullrich and H. Sakai, Thin Solid Films, 423, 273-276(2003).
https://doi.org/10.1016/S0040-6090(02)01037-4
[15] A. Wei, J. Liu, M. Zhuang, Y. Zhao, Mater. Sci. Semicond. Process. 16, 1478-1482 (2013).
https://doi.org/10.1016/j.mssp.2013.03.016
[16] M. Sreedhar, I. Neelakanta Reddy, P. Bera, T.S. Shyju, C. Anandan, Surf. Interface Anal. (2016).
https://doi.org/10.1002/sia.6130
[17] N.M. Saeed, J. Al-Nahrain Univ. 14, 86-92 (2011)
https://doi.org/10.22401/JNUS.14.2.10
[18] Sakhil, M.D., Shaban, Z.M., Sharba, K.S., Habub, N.F., Abass, K.H., Chiad, S.S., Alkelaby, A.S., NeuroQuantology, 18 (5), 56-61 (2020).
https://doi.org/10.14704/nq.2020.18.5.NQ20168
[19] Ghazai, A.J., Abdulmunem, O.M., Qader, K.Y., Chiad, S.S., Habubi, N.F., AIP Conference Proceedings 2213 (1), 020101 (2020).
https://doi.org/10.1063/5.0000158
[20] Khadayeir, A.A., Jasim, R.I., Jumaah, S.H., Habubi, N.F., Chiad, S.S., Journal of Physics: Conference Series,1664 (1) (2020).
https://doi.org/10.1088/1742-6596/1664/1/012009
[21] J. H. Bang, R. J. Hehnich and K. S. Suslick, Adv. Mater., 20, 2599(2008).

https://doi.org/10.1002/adma.200703188
[22] U. P. Gawai, U. P. Deshpande, and B. N. Dole, RSC Adv. 7, 12382-12390 (2017). https://doi.org/10.1039/C6RA28180J
[23] B. E. Warren, X-ray Diffraction, Addision-Wesly Publishing Co., London, (1969).
[24] Hadi, E.H., Sabur, D.A., Chiad, S.S., Habubi, N.F., Abass, K.H., Journal of Green Engineering, 10 (10), 8390-8400 (2020).
[25] Hussin, H.A., Al-Hasnawy, R.S., Jasim, R.I., Habubi, N.F., Chiad, S.S., Journal of Green Engineering, 10(9) 7018-7028 (2020).
[26] M. R. A. Bhuiyan, M. A. A. Azad, S. M. F. Hasan, Indian Journal of pure and Applied Physics, 49, 180-185(2011).
[27] G.K. Williamson, R.E. Smallman, Philosophical Magazine, 1, 34-45(1956). https://doi.org/10.1080/14786435608238074
[28] Ali, R.S., Mohammed, S.A.A., Mohammed, A.H., IOP Conference Series: Materials Science and Engineering, , 928(7), 072154 (2020). https://doi: 10.1088/1757-899X/928/7/072154
[29]Sulaiman, H.T., Ali, R.S., Khoudhair, M.J., Mohammed, S.A.A. NeuroQuantologythis, 18(1), 99–10 (2020). https://doi: 10.14704/nq.2020.18.1.NQ20113
[30] Latif, D.M.A., Chiad, S.S., Erhayief, M.S., Abass, K.H., Habubi, N.F., Hussin, H.A., Journal of Physics, Conference Series 1003(1) 012108 (2018). https://doi.org/10.1088/1742-6596/1003/1/012108
[31] Othman, M.S., Mishjil, K.A., Rashid, H.G., Chiad, S.S., Habubi, N.F., Al-Baidhany, Journal of Materials Science: Materials in Electronics, 31(11), 9037-9043 (2020). https://doi.org/10.1007/s10854-020-03437-0
[32] J. Hasanzadeh, A. Taherkhani and M. Ghorbani, Chinese journal of physics, 51 (3), 540-550(2013).
[33] A.S. Hasan, N. B. Hasan, A. J. Hayder, The first scientific conference for college of science, University of Karbala, pp.18-25(2013).
[34] H. K. Sadekar, N. G. Deshpande, Y. G. Gudage, A. Ghosh, S. D. Chavhan, S. R. Gosavi, and R. Sharma, Journal of Alloys and Compounds, 453, 519 (2008). https://doi.org/10.1016/j.jallcom.2007.10.123
[35] K. Nagamani, P. Prathap, Y. Lingappa, R. W. Miles, and K. T. R. Reddy, Phys. Procedia, 25, 137-142 (2012).
[36] Ali, R.S., Rasheed, H.S., Habubi, N.F., Chiad, S.S. Chalcogenide Letters, 20(1), pp. 63–72 (2023). https://doi.org/10.15251/CL.2023.201.63
[37] I. V. Pankove, Optical processes in semiconductors, New York: Dover Inc., 36(1971).
[38] E. S. Hassan, A. K. Elttayef, S. H. Mostafa, M. H. Salim and S. S. Chiad. Journal of Materials Science: Materials in Electronics 30 (17),15943-15951 (2019). https://doi.org/10.1155/2014/684317
[39] Salloom, H.T., Hadi, E.H., Habubi, N.F., Chiad, S.S., Jadan, M., Addasi, J.S., Digest Journal of Nanomaterials and Biostructures, 15 (4), 189-1195 (2020). https://doi.org/10.15251/DJNB.2020.154.1189
[40] S. H. Mohamed, J Phys D Appl Phys, 43, 035406(2010). https://doi.org/10.1016/j.phpro.2012.03.062
[41] R. S. Ali, M. K. Mohammed, A.A. Khadayeir, Z. M. Abood, N. F. Habubi and Chiad, S.S. Journal of Physics: Conference Series, 1664 (1), 012016 (2020). https://doi:10.1088/1742-6596/1664/1/012016
[42] Chiad, S.S., Noor, H.A., Abdulmunem, O.M., Habubi, N.F., Jadan, M., Addasi, J.S., Journal of Ovonic Research, 16 (1), 35-40 (2020).
[43] Tauc J, ed. Amorphous and Liquid Semiconductor. New York: Plenum Publishing, 441, (1971).
[44] Y. Caglar, M. Caglar, S. Ilican, Current Applied Physics,12, 963(2012).

https://doi.org/10.1016/j.cap.2011.12.017
[45] Jandow, N.N., Othman, M.S., Habubi, N.F., Chiad, S.S., Mishjil, K.A., Al-Baidhany, I.A., Materials Research Express, 6 (11), (2020).
https://doi.org/10.1088/2053-1591/ab4af8
[46] Hassan, E.S., Qader, K.Y., Hadi, E. H., Chiad, S. S., Habubi, N. F., Abass, K. H., Nano Biomedicine and Engineering, 12(3), pp. 205-213 (2020).
https://doi.org/10.5101/nbe.v12i3.p205-213
[47] Ali, R. S. N. A. H. Al Aaraji, E. H. Hadi, Habubi, N. F. and Chiad, S.S. Journal of Nanostructuresthis link is disabled, 10(4), 810–816 (2020).
https://doi: 10.22052/jns.2020.04.014
[48] Chiad, S.S., Alkelaby, A.S., Sharba, K.S., Journal of Global Pharma Technology, 11(7), 662-665 (2020).
[49] Ahmed, N.Y., Bader, B.A., Slewa, M.Y., Habubi, N.F., Chiad, S.S., NeuroQuantology, 18(6), 55-60 (2020).
https://doi.org/10.14704/nq.2020.18.6.NQ20183
[50] B.J. Lokhande, P.S. Patil, M.D. Uplane, Phys. B 302/303, 59-63(2001).
https://doi.org/10.1016/S0921-4526(01)00405-7
[51] A. Jrad, T. Ben Nasr, N. Turki-Kamoun, Optical Materials, 50, 128(2015).
https://doi.org/10.1016/j.optmat.2015.10.011